Design and actual performance of a super high R/C smokestack on soft ground

Shinichiro Mori [a] **M.EERI**

Dynamic analysis considering soil-pile-structure interaction was adopted for the seismic design of a super high reinforced concrete smokestack supported by pile foundation on a reclaimed soft ground in Osaka, Japan. After construction, a series of vibration tests and microtremor measurements were conducted. Moreover, the seismic array observation was carried out to successfully obtain the records during various earthquake events including the 1995 Kobe earthquake. The objectives of this paper are to show the modeling and features of the dynamic analysis model for the seismic design, and to verify the model based on the vibration tests and the seismic observation. The seismic design model is a coupled lumped-mass model consisting of pile-structure and soil systems combined with springs representing the effect of interaction. The analytical results show very good match with the observation results, in terms of transfer functions, time histories and shifted natural periods due to irreversible nonlinear behavior.

INTRODUCTION

A 200 m high reinforced concrete smokestack supported by a long-pile foundation system was constructed on a reclaimed soft ground in Osaka, Japan. Prior to the seismic design of the smokestack, the predominant periods of the ground and the structure were estimated to be long and have been found to become longer under severe seismic motions. It was worried that some transient resonance between the ground and the structure might occur and due to excited nonlinear behavior of soils, unexpected stresses might be produced by the amplified ground displacement. Therefore, it was necessary to study the inertial and kinematic interactions between the soft ground, the pile foundation and the smokestack well during the seismic design. The main objective of this paper is to verify the dynamic nonlinear soil-structure interaction (SSI) analysis model for the seismic design based on the vibration tests and seismic observations. First, an overview of the seismic design of the smokestack and the models of the dynamic analyses for the seismic design is described featuring their

[a] Ehime University, 3 Bunkyo, Matsuyama, Ehime 790-8577 Japan

dynamic characteristics. Second, vibration tests carried out after the construction are discussed especially from the standpoint of the transfer functions between the ground and the structure under very small amplitude vibration. Third, seismic observation results including those during the 1995 Hyogo-ken Nanbu earthquake (also known as the Kobe earthquake) are discussed from the standpoint of the nonlinear behaviors of the ground and the smokestack. Finally, the design models are verified by comparing the results in terms of the time histories of responses of the ground and the smokestack and the transfer functions (i.e., spectral ratios) obtained from the analysis and actual measurements.

In particular, the effectiveness of a simple lumped mass-beam-spring model for the nonlinear SSI analysis in practice is emphasized. So, it may be appropriate to review some typical previous research literatures. Uchida et al. (1980, 1981) analyzed the strong motion records obtained during two big earthquakes in 1978 on an 18-story building made of steel and reinforced concrete, and conducted the elasto-plastic dynamic analysis so as to clarify the change of its natural period during the two earthquakes. Likewise, for Onto Millikan Library in California, four series of vibration experiments were conducted from 1966 to 1969 prior to the 1971 San Fernando earthquake, and another five series of experiments were also carried out from 1971 to 1975 after the earthquake (Luco et al., 1987). Foutch and Jennings (1978), based on their experimental results, clarified the fact that the resonant frequency of a hospital building decreased while the displacement amplitude of its top increased. Moreover, they asserted that this was because of the degradation of the rigidity related to soil-structure interaction during the earthquake motion. In contrast, Luco et al. (1987) asserted that the change of the resonant frequency was not because of the degradation of the rigidity related to the soil-structure interaction but because of the degradation of the rigidity of the super-structure. Celebi (1997) examined the behavior of the six-story Olive View Hospital during the 1987 Whittier earthquake and the 1994 Northridge earthquake using the acceleration records. He clarified that the fundamental frequency of the hospital decreased more significantly during the 1987 earthquake (0.91g in PGA) than the 1994 earthquake (0.061g in PGA). Li and Mau (1997), on the other hand, conducted a system identification analysis and discussed the change of the natural frequencies of 21 buildings where the 1987 Whittier and the 1989 Loma Prieta earthquake records were obtained. Ohba and Hamakawa (1997) also attempted to find the cause of changes of natural periods of buildings that suffered damage to the superstructure or the foundation piles due to the excitation of the Kobe earthquake based on a series of microtremor measurements at the buildings. The

researches mentioned above are thus limited to studying the change in natural period of the structures after experiencing strong earthquake motions. However, investigations related to the change in natural period of the structures occurring right before and after the strong motions are lacking.

OVERVIEW OF THE SEISMIC DESIGN OF THE SMOKESTACK

The 200 m high smokestack for Nanko LNG thermal power plant of Kansai Electric Power Company was erected on a soft manmade island, often known as Osaka Nanko, in 1990. The Nanko Power Plant site can be characterized as a manmade island reclaimed on a very soft thick deposit requiring a long-pile foundation for the structure and having a predominance of longer period components during the earthquakes due to deep Osaka basin. Therefore, the soil-structure interaction between the thick soft soil layer and the super-high smokestack supported on the pile foundation and the pile stress due to ground displacement required careful study and evaluation during the seismic design (Kida et al. 1992). The author worked in the seismic design of the smokestack as a leading engineer from 1987 to 1989. A bird's eye view of the smokestack is shown in Photo 1.

Photo 1. Bird's eye view of the smokestack of Nanko Thermal Power Plant of KEPCO (By courtesy of KEPCO)

The location of the site is such that it lies on a reclaimed land near the Osaka Bay area and at almost the center of the basin surrounded by the mountains, as shown in Figure1. From the viewpoint of earthquake ground motion, 3 to 4 period components tend to be predominant in Osaka City area, which is considered to be due to the surface wave induced by the basin effect of the Osaka Basin. The strongest ground motion experienced at the site during the 1995 Kobe earthquake with an epicentral distance of about 22 km will be discussed later.

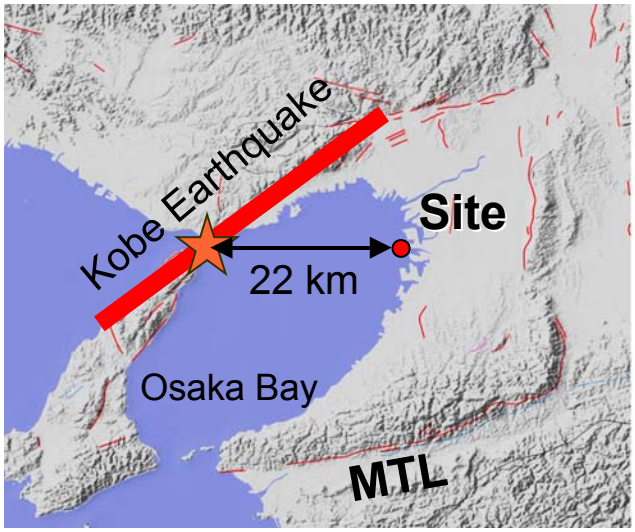

Figure 1. Location of the site and the epicenter of the 1995 Kobe earthquake

Figure 2 shows the front and side views of the smokestack together with the arrangement of the accelerometers on the smokestack as well as the ground. The smokestack consists of three internal cylinders made of FRP and an external hexagonal reinforced concrete structure supporting the cylinders. The height of the internal cylinders is 200m and that of the external structure is 194m. The cross section of the external structure is a hollow hexagon with two different sides attached with three pairs of straight wings, and the outline of vertical figure follows a straight line and a parabolic curve. The width of the wings decreases gradually from 8.0 to 3.1 m toward the top of the smokestack while the maximum internal width of the hexagon decreases from 18.5 to 13.1 m, and the wall thickness decreases from 100 to 30 cm. Near the bottom of the smokestack, three openings exist for horizontal penetration of the smoke pipes connected to the internal cylinders. Each opening has a length of 10 m and a width of 8m, and is located at 5 m above the base of the smokestack. The external structure was constructed by slip-form concrete method such that it supports the internal FRP cylinders at 18 and 177 m of elevation points.

The accelerometers, as indicated in Figure 2, consist of two horizontal component accelerometers fixed at 65, 131, and 193.5 m height on the smokestack, and a three component accelerometer on the smokestack base. The aim of fixing the accelerometers is to measure the third vibration mode of the smokestack. Two additional vertical accelerometers on the base aimed for extracting two-directional rocking of the base were incorporated with one on it. A pair of three component accelerometers was also installed at the depths of 1 m and 70 m below the ground so as to measure the principal behavior of a free field 100m away from the smokestack.

The plan and elevation of the smokestack base along with the arrangement of 273 piles are show in Figure 3. The piles are seen concentrated near the edges of the basement with at least 2-meter interval for effectively resisting the rocking of the base. Each pile is made of five segments consisting four pre-stressed high strength concrete piles (PHC piles) and one

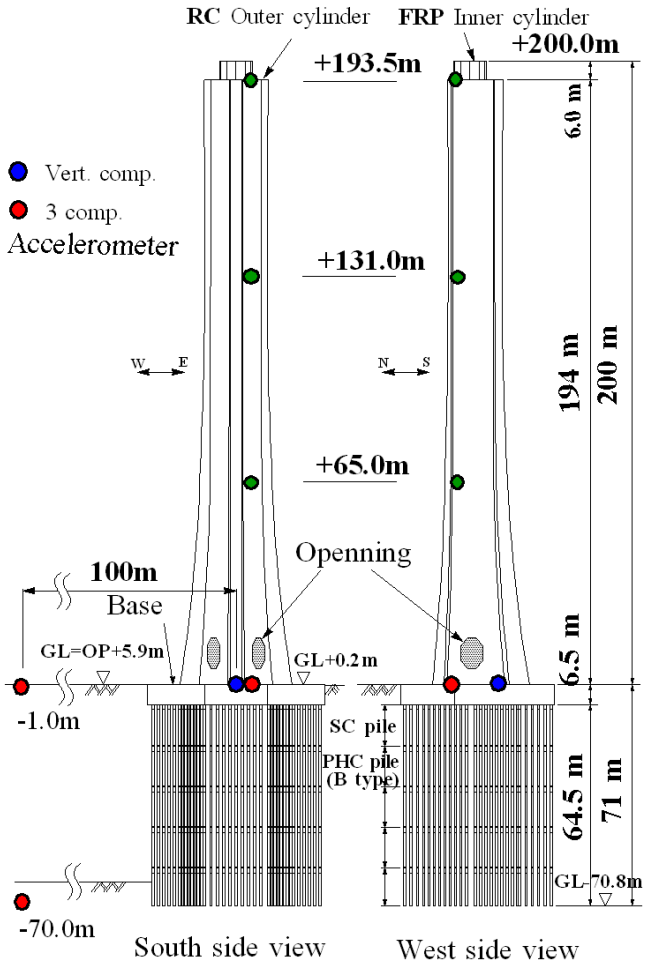

Figure 2 Front and side views of the smokestack and the arrangement of accelerometers on it and on the ground

steel reinforced PHC pile (B-type: the second strongest) on the top with an external diameter of 80 cm. Each pile has a length of 65 m and reaches the pile base layer composed of second dilluvial gravely sand at a depth of 72 m. All the piles penetrate the soft and hard layers, so there was an anxiety during the construction that seismic ground displacement could induce some stress concentration in the piles near the boundaries between the soft and hard layers. The base of the smokestack measures 6.5 m deep and 51 m wide having sufficient rigidity against rocking.

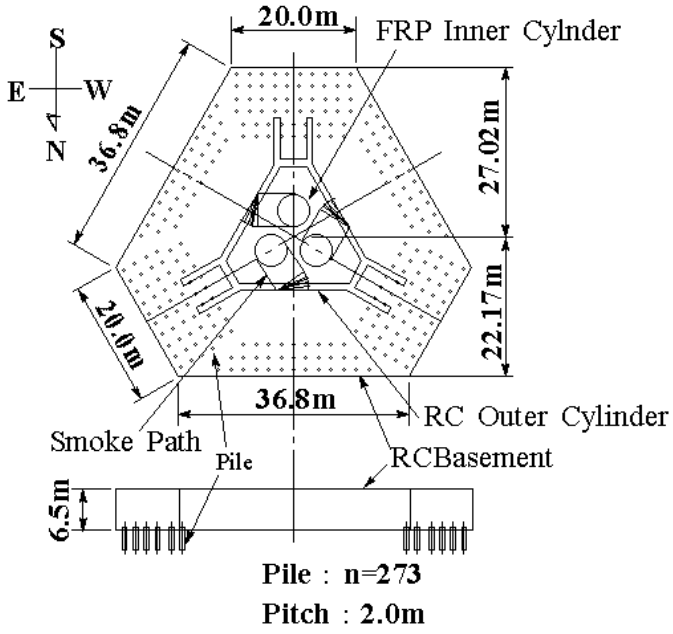

Figure 3. Plan and side views of the basement and the arrangement of 273 piles

The detailed soil profile at the site is shown in Figure 4 together with the SPT N-values and shear wave velocity profiles. The soil profile consists of different layers, which include 6.5 m thick banked layers, 10.7 m thick filled layer, 25.5 m thick alluvial clay-silt-sand layer (Ma13), 8 m thick dilluvial gravel layer (Temma Layer), 14.5 m thick dilluvial clayey layer (Ma12), and 11 m thick second dilluvial gravely sand layer. The base for the piles was selected to be 11 m thick second dilluvial gravely sand layer. The reclamation work was carried out in 1972 through 1980. The banked layers were filled with the material exploited from the mountains and waste soil from the construction sites after the lower layer was dredged and sand drains were applied for consolidation of alluvial clayey layer.

The performance requirements for the seismic design of the smokestack were specified

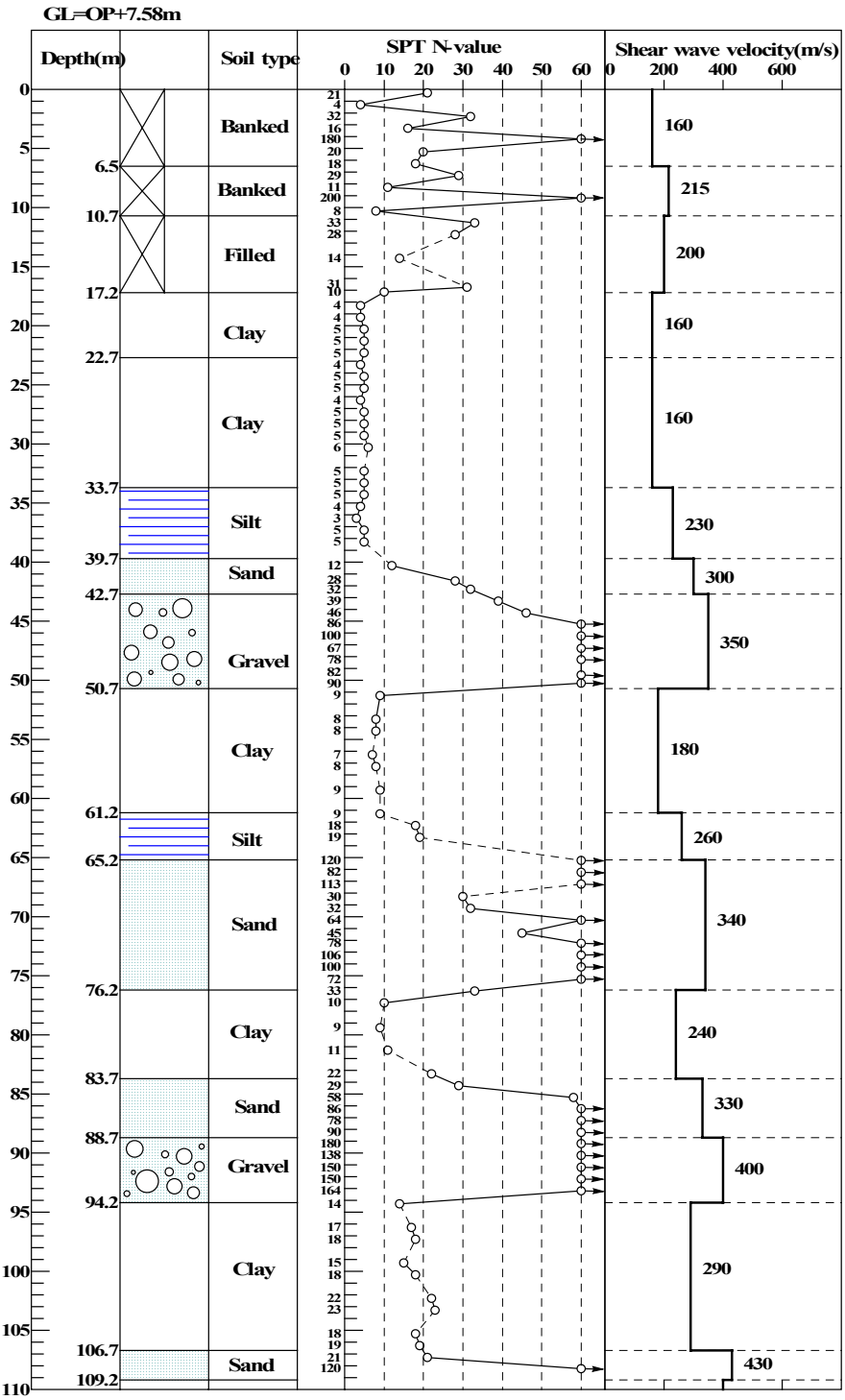

Figure 4. Soil profile at the site including SPT N-value and shear wave velocity profiles

for two levels of earthquake motion: 1) serviceability during and after the Level 1 motion and 2) safety during and after the Level 2 motion. The maximum velocities of ground surface for the Level 1 and 2 motions were evaluated to be 25 and 50 cm/s respectively. The input

ground motions for the dynamic response analysis for the seismic design were basically defined as surface ground motion of the free field because a fixed base model was adopted as a basic model of dynamic analysis as per the Japanese conventions. Basically, four strong motion acceleration time histories including El Centro (NS), Taft (EW), and Hachinohe (NS) records, as per the conventions, were adopted as input motions with scaled amplitude in the previously mentioned velocities. The major performance criteria were the ductility factor and allowable shear stress for the smokestack, the allowable tensile stress for the internal FRP cylinders, and the allowable stresses for the foundation base and the piles. The criterion of the ductility factor with regard to the Level 2 motion was 2.0, which resulted in a ductility factor of 1.45 in the maximum response for the Level 2 motion with Hachinohe record, which is rich in longer period components. The ground was assumed to be a horizontally layered system during the analysis, and three different ground models were prepared in terms of the degree of non-linearity of soils, as shown in Figure 5.

The basic ground model, which is assumed to have a set of rigidity determined based on

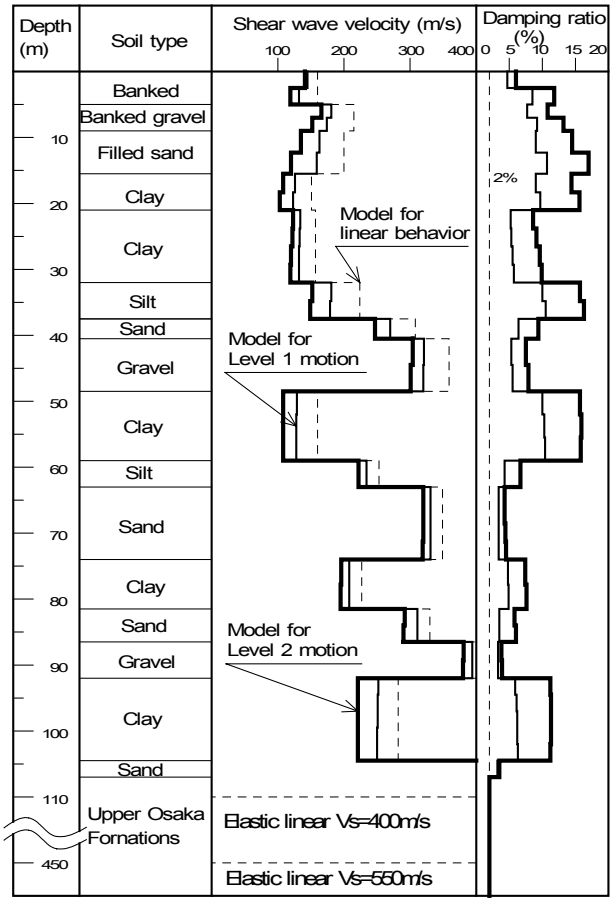

Figure 5 Three different ground models depending on the degree of non-linearity of soil

the PS logging at the site, is regarded as an elastic linear ground, and is used in the analysis for the ground motions with small amplitude. The other two models have different values of rigidity and damping ratio under the Level 1 and 2 motions. The values were determined as an average of three convergent values in the cases of equivalent analyses with El Centro, Taft, and Hachinohe as the input motions by using SHAKE program. Each analysis was repeated until the surface velocity response converged to the given magnitude of Level 1 or 2 motions. Figure 5 shows the shear wave velocity and damping ratio profiles of these three different models of the ground. The magnitudes of predominant strain in the seismic grounds ranged from 0.03 to 0.2 % for the Level 1 motion and from 0.05 to 5 % for the Level 2 motion.

MODELS OF DYNAMIC ANALYSES FOR THE SEISMIC DESIGN

Generally, a fixed base model is adopted for seismic design when the effect of soil-structure interaction is considered negligible. When this effect is taken into account, the use is commonly made of a sway rocking model for the structures with spread or short-pile foundation. The SSI effect on the structure as well as piles, however, is considered significant in case of long piles in soft ground. In such a case, some coupled system should be adopted for the seismic design model. A finite element model would be powerful in evaluating the SSI effect if it were linear. Unfortunately, however, it was not available for the structural and geotechnical nonlinear models at that time. So, a lumped mass-spring-beam model was

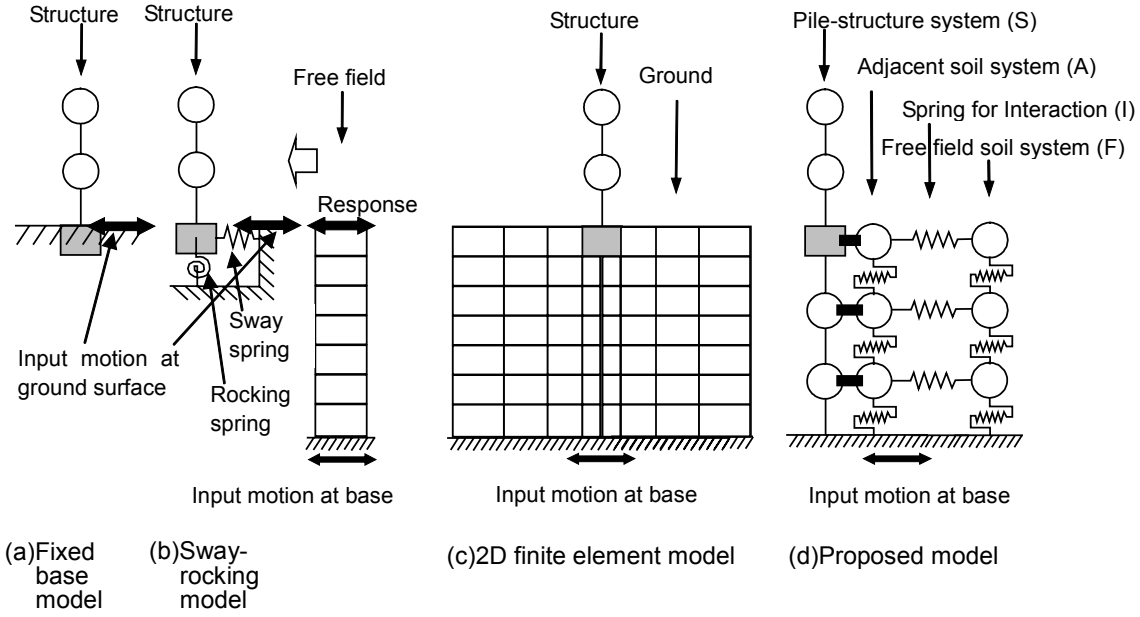

Figure 6 Models of preliminary analyses as candidates for the seismic design

considered appropriate for taking into account the major SSI effect as well as the material non-linearity in the structure and the ground. As a result, the author and one of his colleagues developed and proposed the lumped mass-spring-beam model (Mori et al. 1992; Mori 2000). Figure 6 shows the models mentioned above.

In order to evaluate the appropriateness of the above-mentioned models in the seismic design, preliminary analyses employing these models with the soil properties in the Level 1 motions were conducted, and the results from the different models were compared. The three of the four actual models employed in the preliminary analyses are shown in Figure 7 for reference. In addition, the modified FLUSH model was studied.

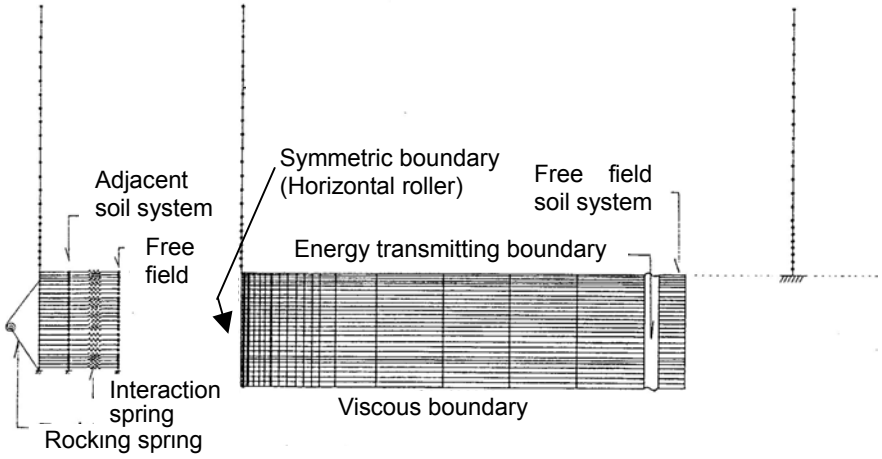

(a) Proposed model (b) 2D FEM(FLUSH) model (c) Fixed base model

Figure 7 Three of four actual models for the preliminary analyses

As the basic information, the predominant periods of the smokestack obtained from the above-mentioned models are given in Table 1. In 2D-FEM model, the predominant periods are specified by its transfer function of the top of smokestack to the base of the ground. In the rest of the models, however they are specified according to the result of eigenvalue analysis.

Table 1 Predominant periods of the smokestack

Type of model	1st	2nd	3rd		4th	
			Rocking	Sway	Rocking	Sway
Fixed base model	2.22	0.49	0.20		0.1	
Sway-rocking model	2.33	0.54	0.21	0.25	0.13	
Lumped mass-spring-beam model	2.33	0.54	0.21	0.29	0.12	0.11
2D-FEM model	2.38	0.58	0.23		0.12	

Note1: SSI models are based on the soil properties assumed under Level 2 earthquake motions
Note2: The detail of the smokestack for preliminary analyses was different from the final structure.

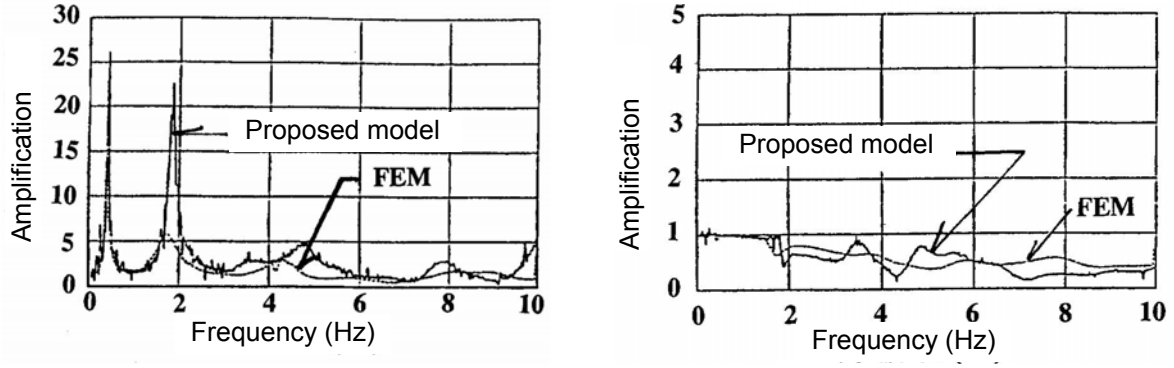

(a) Top of smokestack (b) Basement

Figure 8 Transfer functions of the top of the smokestack and of the basement to the ground surface of the free field with regard to horizontal movement

The transfer functions in the amplitude, i.e., Fourier spectral ratios, of the top of the smokestack and its base to the ground surface of the free field and to the ground surface with regard to horizontal movement as obtained from the proposed model and the two dimensional FEM model are compared in Figure 8 (a) and (b). As for the transfer functions of the top of the smokestack, the predominant periods of the first and second modes in these two models match well. However, the amplification near the second predominant period for the smokestack from the proposed model is much greater than that from the FEM model, whereas it is only slightly greater over the frequency ranges beyond the second predominant period. The 2D FEM model may overestimate the dissipation damping of the smokestack, so the proposed model was considered more appropriate in the practical seismic design. As for the transfer functions of the smokestack base, the input loss effects due to kinematic interaction are simulated in the similar manner, and the results in terms of phase differences are shown in Figure 9. The results from both the models are seen to match well as a whole.

On the other hand, the sway-rocking model for the smokestack was not adopted for the dynamic analysis model for the seismic design, because of great discrepancy with the FEM

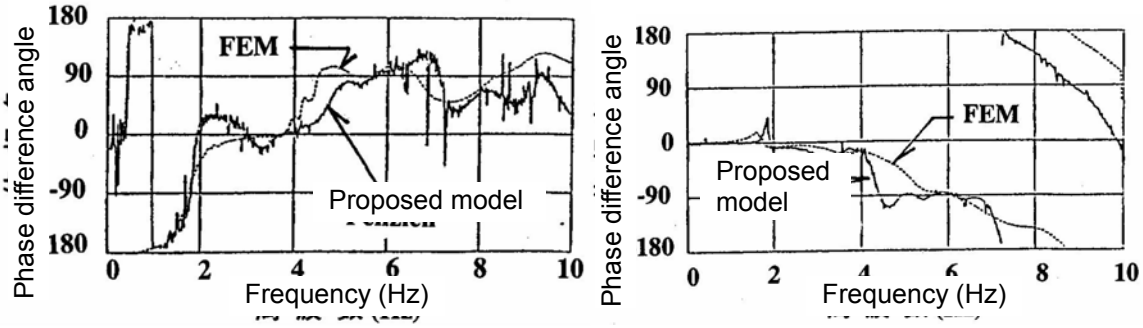

Figure 9 Transfer functions in phase difference of the top of the smokestack and of the basement to the ground surface of the free field with regard to horizontal movement

model near and beyond the second predominant frequency in the above-mentioned transfer functions both in amplitude and phase difference.

In order to understand the natural modes in the proposed model, some lower vibration modes of the proposed model together with those of the fixed base model are shown in Figure 10. As shown in the figure, the modes of sway and rocking of the foundation are clearly recognized and excited modes and amplitudes of the smokestack in the periods of predominant or natural ground vibration can be quantitatively understood (Mori 2000).

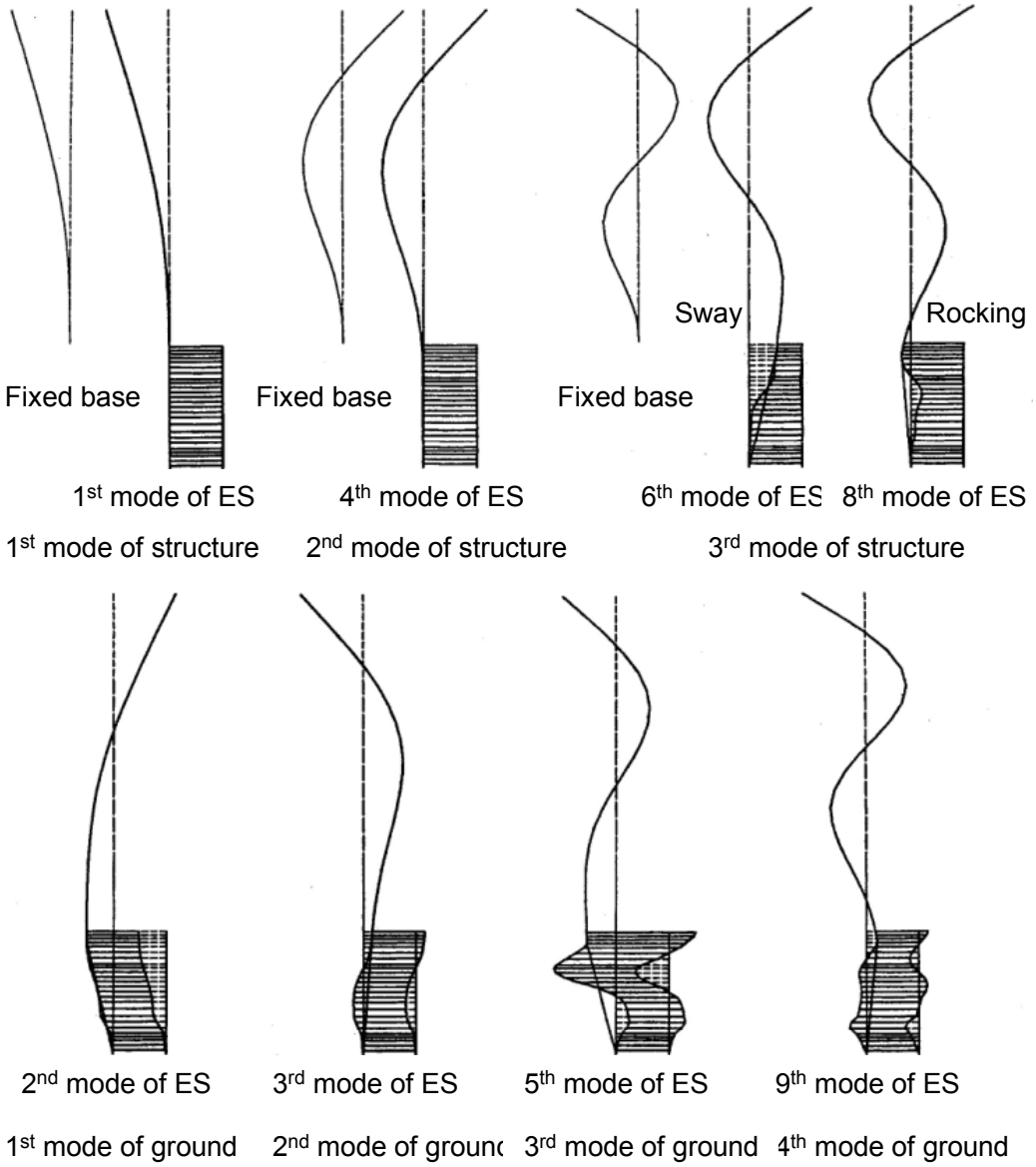

Figure 10 Lower vibration modes of the proposed model, which can be identified to the specific modes of the ground, the structure, or the foundation

VERIFICATION OF THE MODELS BASED ON VIBRATION TESTS

A series of vibration tests including microtremor measurements and artificial excitation (i.e., by the use of human power) tests were carried out just after the construction in August 1990 (Kida et al. 1992). The artificial excitation for the first natural period of the smokestack

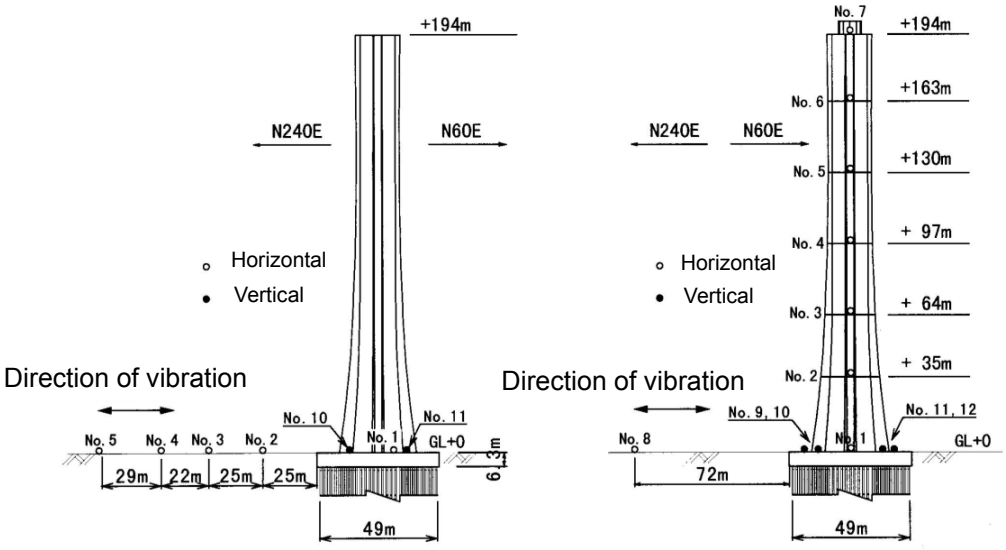

(a) For measurement of the ground (b) For the measurement of the smokestack

Figure 11 Arrangements of sensors for the ground and the smokestack

was produced by a cyclic movement of individual centers of gravity of 27 persons on top of the smokestack, while that for the second natural period was produced by applying a joint push of 12 persons on the wall at the top. In order to find a point that could be regarded as the free field for the smokestack-ground system, array observation of microtremor was also carried out. Figure 11 shows the arrangement of the sensors (velocity meters) for the ground and the smokestack during the tests. Figure 12 shows the Fourier spectra of the ground surface and the base of the smokestack, which indicates a gradual decrease of the amplitude

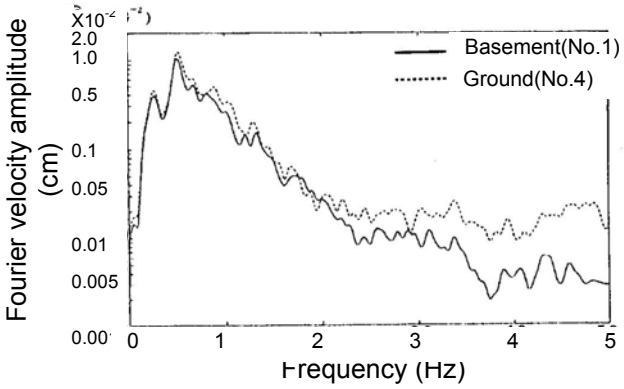

Figure 12 Fourier spectra of the ground surface and the basement

of the base in higher frequency compared with the ground surface. Moreover, the spectral ratios of the base to the ground surface obtained from the microtremor measurements as well as the analysis by the proposed method are shown in Figure 13(a). This figure clearly shows the input loss effect due to kinematic interaction, which can be successfully simulated by the analysis using the proposed model. Moreover, the transfer functions with regard to rocking of the smokestack base to the horizontal ground surface motion, as obtained from the measurement and the analysis are compared in Figure13(b). This analytical model may underestimate the amplification of the rocking effect due to SSI, especially around the second predominant period.

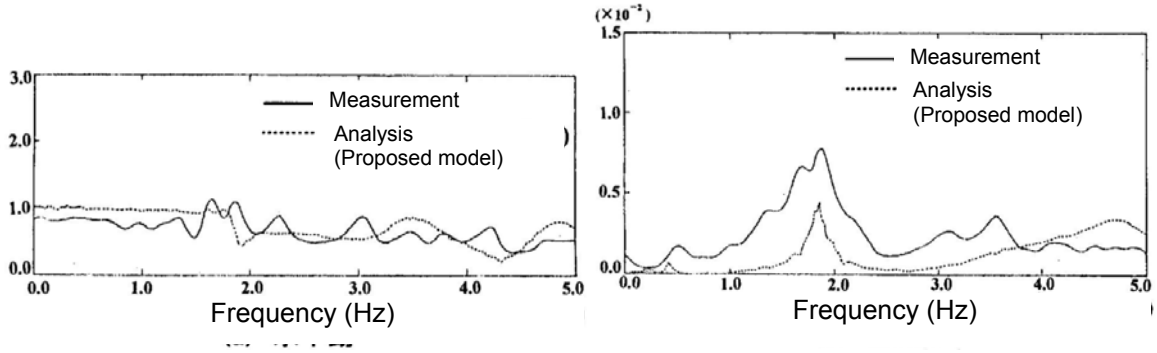

(a) Translation (b) Rotation

Figure 13 Spectral ratios of the basement to the ground surface both by microtremor measurement and the analysis by the proposed method

Next, the transfer functions of the top of the smokestack to the ground surface of the free field as obtained from the microtremor measurement and the analysis using the proposed model with the soil properties under the Level 2 earthquake motions are compared in Figure 14. Two distinctive features can be seen in this figure. First, the predominant frequencies of

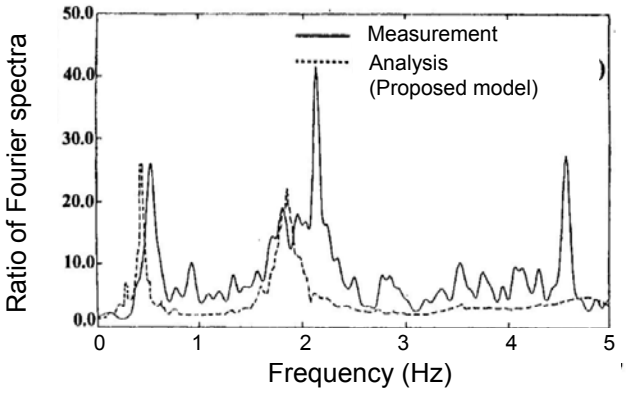

Figure 14 Transfer functions of the top of the smokestack to the ground surface of the free field by microtremor measurement and analysis with the proposed model

the measurement are obviously observed to be greater than those of the analysis around the first and the second predominant frequencies, and the ratios of the measured values to the analytical results are almost the same. Second, the shapes of these two transfer functions are almost proportional. These two features are considered to be due to the difference in dynamic properties of the analytical model and the actual structure. The first predominant frequency does not seem to be strongly influenced by the SSI, which means that the difference may be due to the difference of the flexural rigidity of the smokestack.

Furthermore, a comparison of the first and second vibration modes of the smokestack as obtained from the measurement and the analysis is made in Figure 15. Both the microtremor measurement and the artificial excitation test are seen to have resulted in the same vibration mode except for a slight difference of the predominant frequency of the second mode.

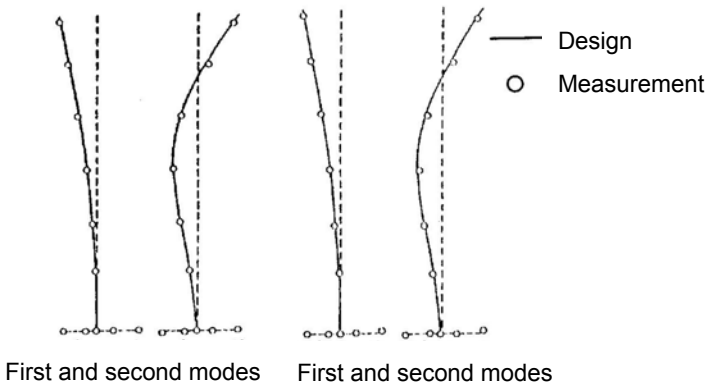

(a) Microtremor measurement (b) Manpower excitation

Figure 15 Comparison of the first and second vibration modes of the smokestack between the measurement and the analysis

Table 2 shows a summary of the predominant periods of the first and second modes as obtained from the analysis and the measurement. The fundamental periods of the smokestack are found to be different. Accordingly, such differences are hereinafter going to be studied

Table 2 Summary of predominant periods of the first and the second mode by the analysis and the measurement

Model and measurement	Top/Free field		Top/Basement	
	1st	2nd	1st	2nd
Fixed base model			2.22	0.49
Proposed model	2.37	0.54		
Microtremor measurement	1.87	0.46	1.89	0.45
Manpower excitation			1.92	0.49

Unit: second

from the standpoint of Young's modulus of concrete. The design value of the Young's modulus of concrete, Ec used in the smokestack was Ec=2.3×10^5 kgf/cm^2, which was estimated by using an empirical relationship between Young's modulus and the strength of concrete considering the design strength of concrete, Fc=240 kgf/cm^2.

The strengths of the actual concrete used in the smokestack are statistically shown in Figure 16. The average compressive strength of the concrete measured at the construction site was 410 kgf/cm^2, and the average Young's modulus can be estimated to be E=3.3×10^5 kgf/cm^2, which was to be applied in the analysis for vibration experiment. The natural periods according to the proposed model with such modification was almost the same as the measured ones.

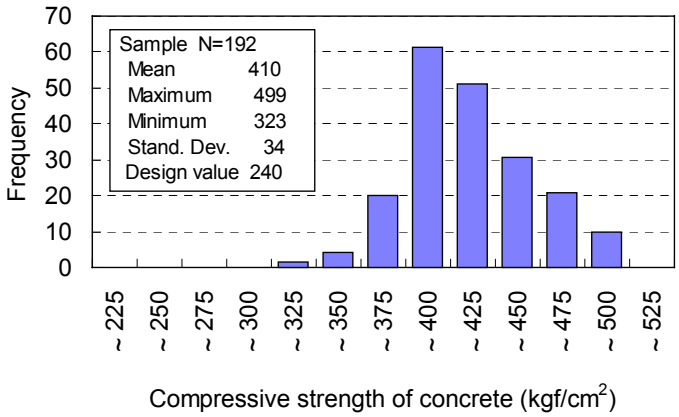

Figure 16 Histogram of the strength of concrete for the smokestack

The damping ratio was measured based on the free damped vibration after the artificial excitation. Figure 17 shows the time history of displacement at the top during the free damped vibration after the artificial excitation. The damping ratio was measured to be approximately 1.1% at all the heights of sensors from the free vibration. Additionally, the damping ratio estimated by the half power method with the microtremor measurement varied from 1.1 to 1.5%, which is almost the same as the value estimated from the artificial

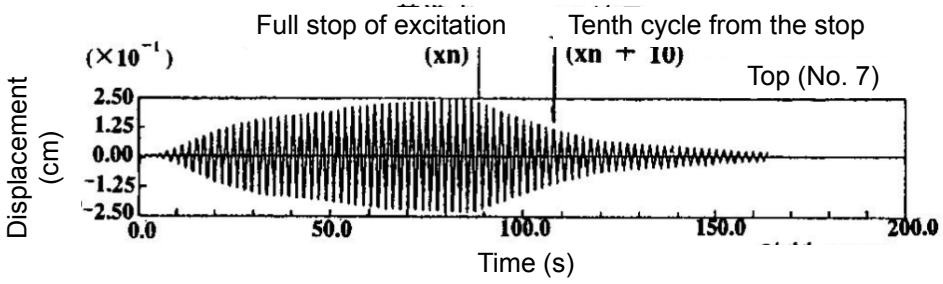

Figure 17 Time history of displacement at the top during the free damped vibration.

excitation. The design value of the damping ratio was 2%, which was considered appropriate taking into account its dependency on the strain.

ACTUAL SEISMIC BEHAVIOR OF THE GROUND AND THE SMOKESTACK

The earthquake observation for the smokestack and the ground was carried out right after the completion of the construction in March 1990. The arrangement of the seismometers has already been mentioned elsewhere. The observations were made until the end of 1997 during twelve earthquakes, the epicenters of which are shown in Figure 18 (Kowada et al. 1997). The ten of these earthquakes were the main event and the aftershocks of the 1995 Kobe earthquake, as mentioned also in conjunction with Figure 1.

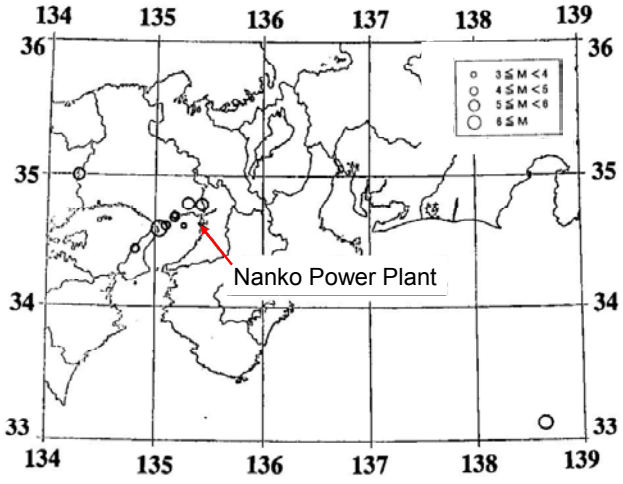

Figure 18 Location of the epicenters of the earthquakes observed at Nanko site

For grasping the overall amplification or de-amplification through the ground, the foundation, and the smokestack, the relationship of the maximum accelerations among the base layer, the ground surface, and the basement and the top of the smokestack are shown in Figure 19. The amplification factor through the subsurface ground is not so great, varying mostly from one to two. From the relationship between the ground surface and the basement of the smokestack, de-amplification can be found especially in the range of low amplitude. This de-amplification can be understood as the effect of input loss due to the kinematic interaction between the foundation ad the ground, whereas this effect is negligible in the case of the main event of the Kobe earthquake. The amplification through the smokestack varies from two to five times, and the factor seems to be greater when the amplitude of the ground surface acceleration is smaller.

The predominant frequencies of the ground and the smokestack were determined based

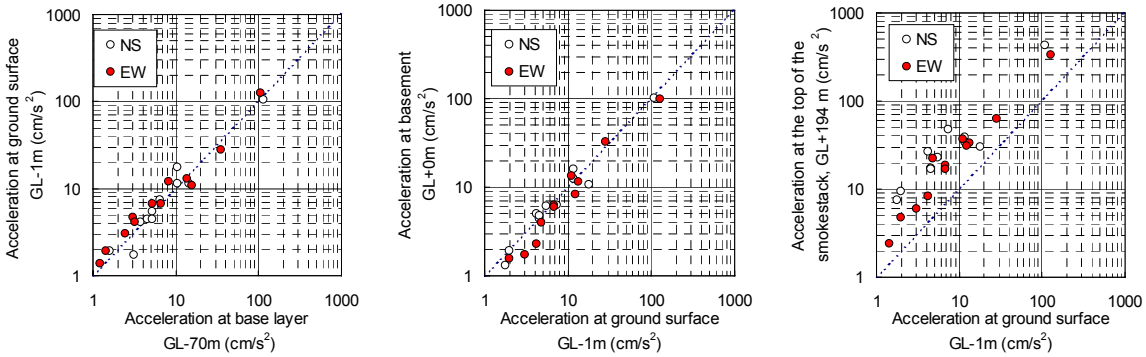

Figure 19 Relationship of the maximum accelerations among the base layer, the ground surface, and the basement and the top of the smokestack

on the predominant peaks in the spectral ratios of the ground surface to the base layer and in those of the top to the base of the smokestack, respectively. Figure 20 shows the relationship between the predominant frequencies and the magnitude of the input in the systems of the ground and the smokestack. The dependency of the predominant frequency on the input to the systems, such as the ground and the smokestack, can not be clearly seen.

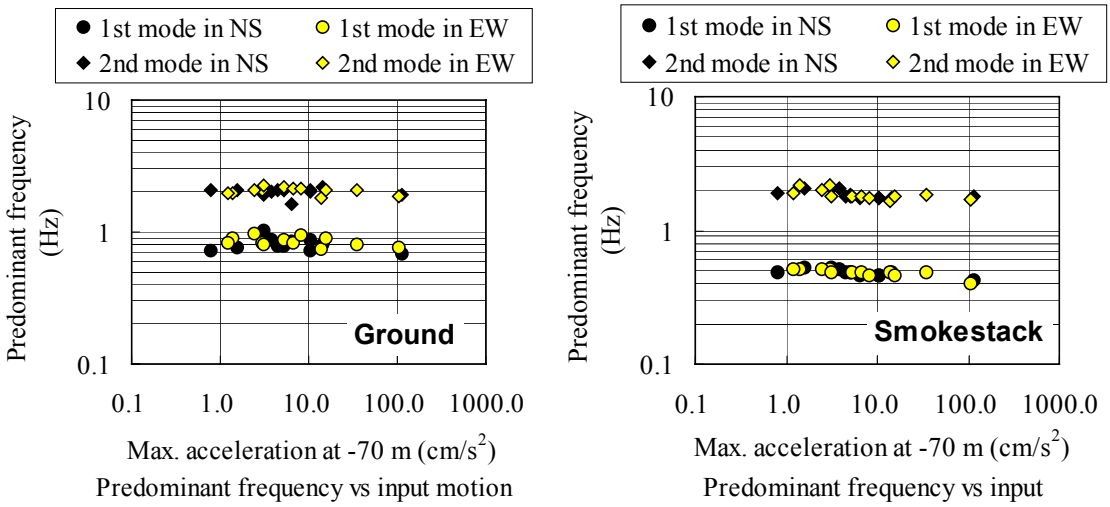

Figure 20 Relationship between the predominant frequencies and the magnitude of the input in the systems of the ground and the smokestack

In order to study the change of the first and second predominant frequencies along the progress of the time, the change of the predominant periods in the order of the time of the earthquakes is shown in Figure 21. As for the predominant periods of the ground, those during the Kobe earthquake are the longest both in the first and second ones, and those after the Kobe are longer than those before the Kobe in the first predominant period, while the

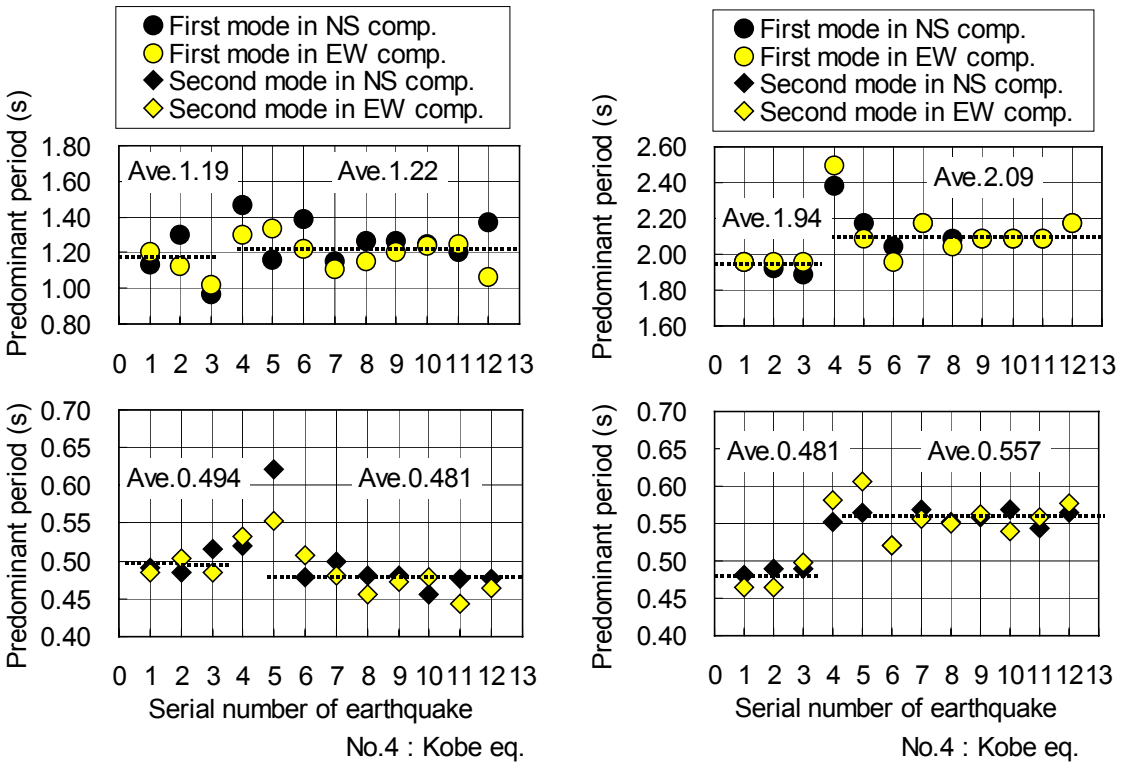

(a) Ground (b) Smokestack

Figure 21 Change of the predominant periods in the order of the time of the earthquakes

reverse relation can be recognized in the second ones. The second predominant period can be considered influenced by the soil properties in relatively shallower soils. Accordingly the excitation by the Kobe earthquake might have densificated the shallower sandy soil deposits. On the other hand, a slight change of the first predominant period toward the longer side can be supposed to be due to the effect of softening in clayey soil deposits in deeper location. As for the predominant periods of the smokestack, the first one during the main event was significantly long, and those after the Kobe are longer than those before the Kobe. The averaged values of the first predominant period before and after the Kobe earthquake are 1.94 and 2.09 seconds, respectively. Moreover, the averaged values of the second predominant period before and after the Kobe are 0.48 and 0.56 seconds, respectively. These irreversible changes of the predominant periods are considered to mean that the stresses in the smokestack had gone far beyond the elastic limit or the cracking limit (Kowada et al., 1998).

VERIFICATION OF THE MODELS BASED ON STRONG MOTION RECORDS

The ground motion observed during the Kobe earthquake is approximately equal to the magnitude of the Level 1 design motions in terms of velocity of the ground surface. In

addition, the behavior of the ground and the smokestack has been clarified to be strongly nonlinear in the previous section. Consequently, the numerical simulation with the record during the Kobe earthquake by the seismic design models including the conventional fixed base model and the proposed model can be suitable verification of the seismic design of the smokestack. Figures 22 and 23 show the time histories of the north-south components of the acceleration and displacement of the ground and the smokestack, respectively. The duration of the principal motions of the ground approximately begins at 16 seconds and ends at 28 seconds, whereas the significant amplitude of vibration when four-second component is highly predominant takes place in the later stage just after the principal motion continues up to 120 seconds in the top of the smokestack. In particular, the maximum displacement of the top takes place in the later stage. This four-second predominant component is also significant

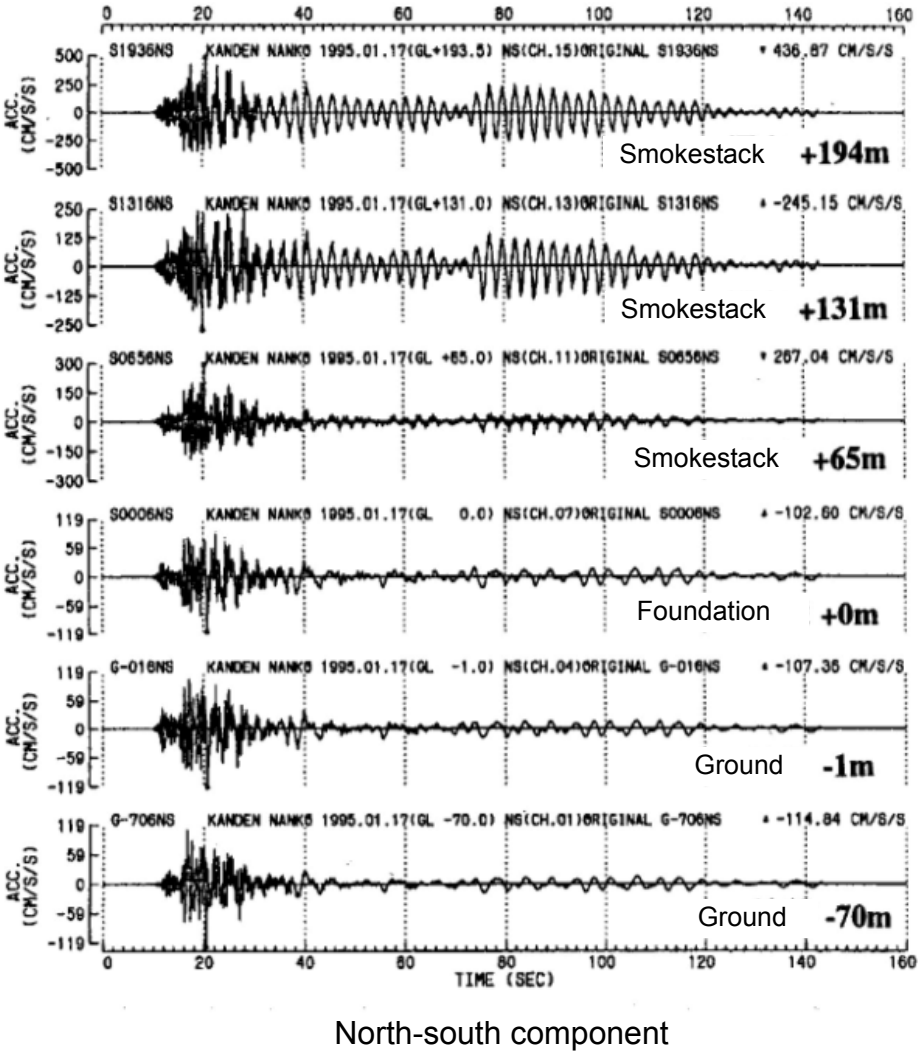

Figures 22 Acceleration time histories of the north-south components of the ground and smokestack

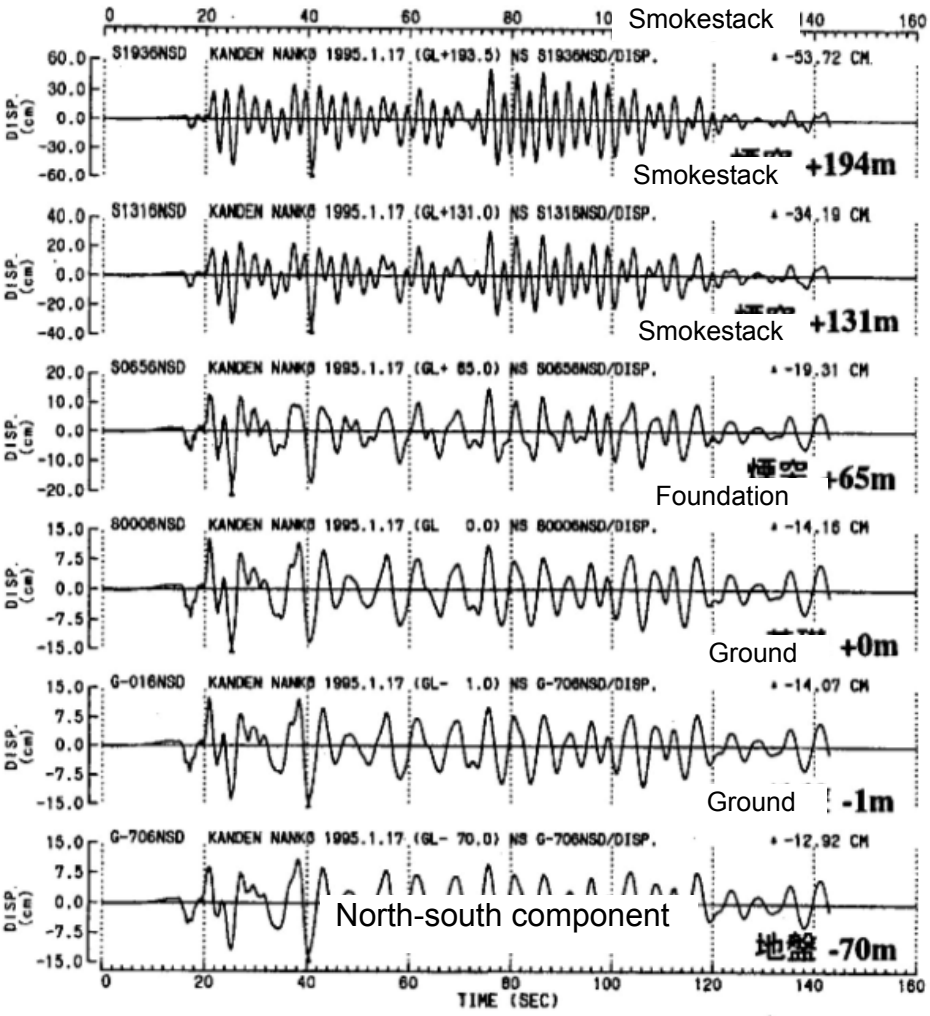

(a) NS成分

in the displacements at the two depths of the ground with almost the same amplitude, which is hence considered to be a kind of surface wave, probably the Love wave.

A numerical analysis was conducted by the proposed model used in the seismic design with the recorded acceleration at the base at a depth of 70 m as the input motion for the models. The analysis by the fixed base model was conducted with the recorded ground surface motion as the input motion. Figure 24 shows the acceleration response time histories of the top of the smokestack, the basement of the foundation, and the ground surface together with the measured ones. The response of the top of the smokestack is focused on the time range of the principal motion because this is thought to be dominated by vertically incident shear wave.

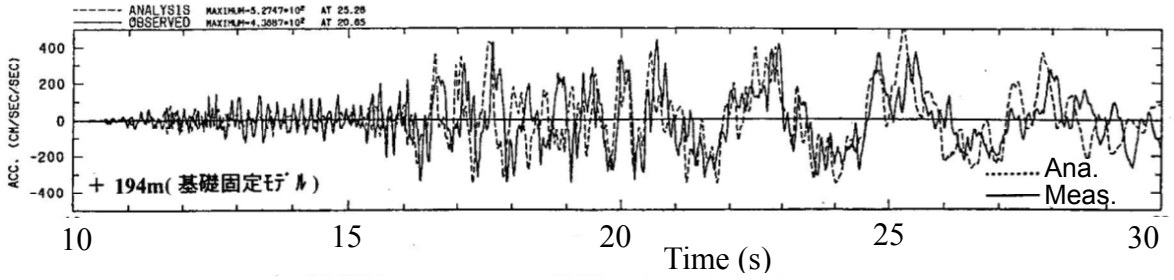

(a) Response of the top of the smokestack by the fixed base model

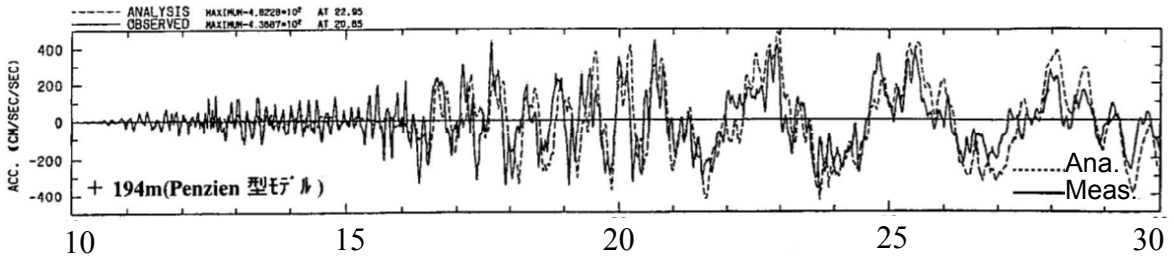

(b) Response of the top of the smokestack by the proposed model

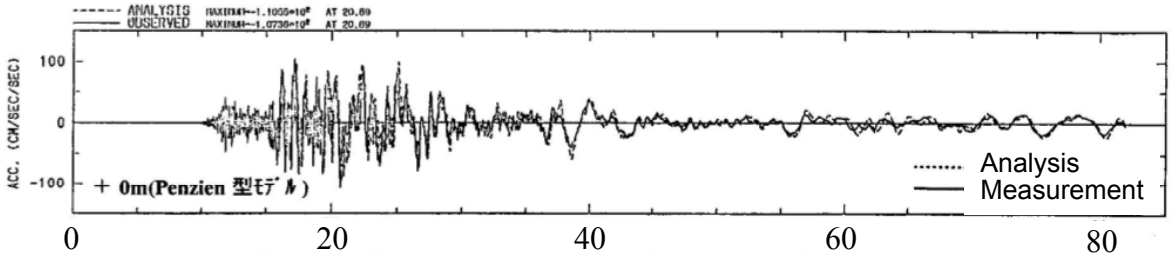

(c) Response of the basement of the foundation by the proposed model

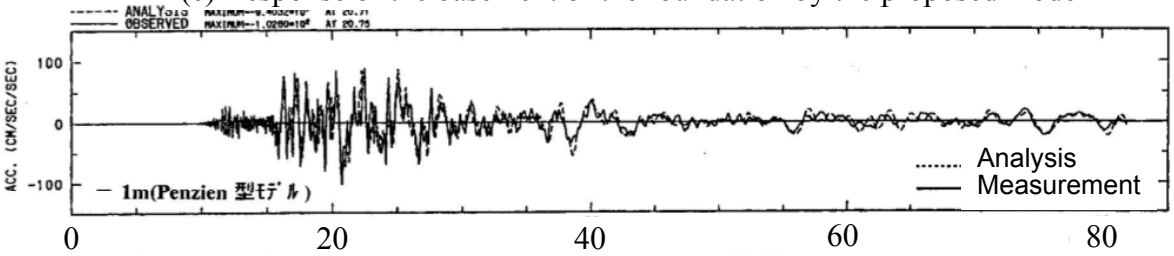

(d) Response of the ground surface by the proposed model

Figure 24 Acceleration response time histories of the top of the smokestack, the basement of the foundation, and the ground surface together with the measured ones, which is focusing on the time range of the principal motion

In the response of the ground surface, a good agreement is seen in Figure 24. Accordingly, the difference of the ground surface motion between the two models may not be so influential to the response of the smokestack. Comparing the waveform of the basement with that of the ground surface, it is clearly understood that the short period components are obviously reduced. As for the degree of this reduction, the measured one is greater than the analytical one, which means the reduction may not be only due to kinematic interaction along the depth but also due to that in the horizontal plain.

As for the response of the top of the smokestack, both the analytical results roughly match the measured one in terms of amplitude and phase; however, the phase in the response of the fixed base model slightly advances more than the measured one, while that of the proposed model well matches the measured one. This means that the response of the smokestack from the motion directly transmitted through the pile foundation is presumably dominant in the entire response of the smokestack and the proposed model is able to simulate this mechanism.

Next, the spectral ratios of the top of the smokestack to the ground surface for the north-south component are shown in Figure 25 in order to discuss soil-structure interaction effect from the viewpoint of the transfer function between them. For the first predominant period, the two analysis results match the measurement. For the second predominant period, the result of the proposed model well matches the measured one, but that of the fixed base model is shorter than the measured one. Additionally, a small peak around 1.2 to 1.3 seconds, which may be due to the effect of the first predominant mode of the ground, can be simulated only by the proposed model but not by the fixed base model.

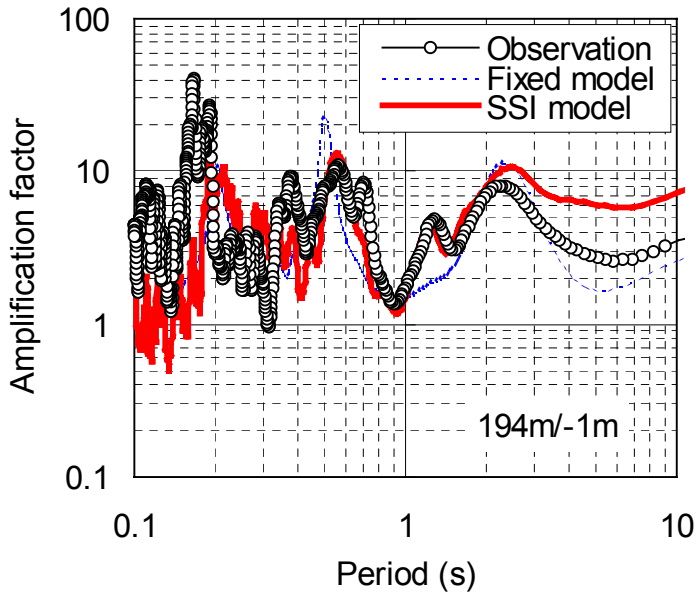

Figure 25 Spectral ratios of the top of the smokestack to the ground surface and to the base layer for the north-south component

Figure 26 shows various kinds of the spectral ratios of the proposed model and the measurement. That of the top of the smokestack to the base layer, which represents the overall dynamic characteristics of the coupled model, matches the measurement result. That of the ground surface to the base layer, which represents the dynamic characteristics of the

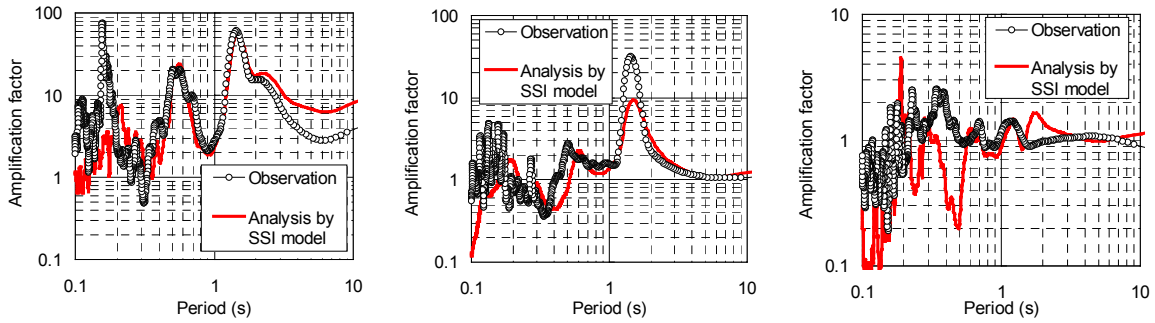

(a)Entire system: Top/GL-70m (b)Ground: GL-1m/GL-70m (c) Basement/GL-1 m

Figure 26 Spectral ratios of the proposed model and measurement

ground, also matches the measurement result. As for that of the basement to the ground surface, which represents the effect of input loss in the foundation, both the shapes are roughly the same, whereas the detailed shapes are different.

Figure 27 shows the maximum responses of bending moment and curvature of the smokestack on the skeleton curves with regard to the direction when the north side of the smokestack is in tension and with regard to the east-west direction. In this figure, the two breaking points of each skeleton curve correspond to the cracking and the yielding surfaces. The yielding surface is defined as a situation when the most outer reinforcement bars start to yield. According to the figure, the response of the smokestack went beyond the cracking surface in the range of heights from 20 to 120 m in case of the proposed model, while such

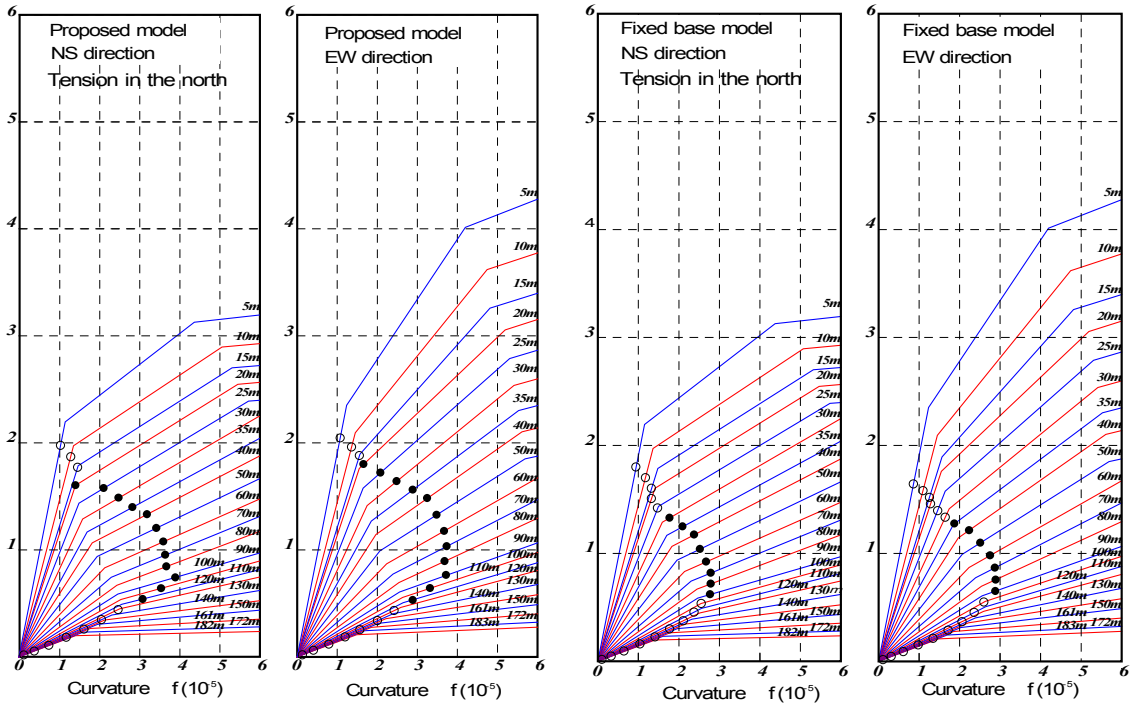

Figure 27 Maximum responses of bending moment and curvature of the smokestack on the skeleton curves

situation occurred in a range of heights from 30 to 90 m. The values of residual rigidity of the smokestack estimated from its changed predominant periods, which was mentioned earlier, might correspond to those in case of the proposed model.

Based on the comparison of the results of the analyses using the proposed model and the measurement with regard to the time histories of accelerations of the ground and the smokestack, the transfer function of the smokestack, and the relationship between the change of the predominant periods and the nonlinear response of stress-strain of the smokestack, the appropriateness and effectiveness of the proposed model can be verified.

CONCLUSIONS

The soil-structure interaction model proposed by Mori et al.(1992) and Mori(2000) was adopted in the seismic design of a 200 m high reinforced concrete smokestack constructed on a soft ground in Osaka, Japan. The fundamental dynamic characteristics of the smokestack were examined by microtremor measurements and manpower excitation tests with regard to its elastic behavior. Moreover, the earthquake observations on the ground and the smokestack were carried out, and the strong motion records during the 1995 Kobe earthquake were analyzed and used in the numerical analyses with the seismic design models. The results of a series of tests on the elastic behavior and the numerical simulation on the nonlinear behavior of the ground and the smokestack could verify the appropriateness of the proposed model as the seismic design model and its effectiveness as a nonlinear SSI analysis model qualitatively as well as quantitatively.

ACKNOWLEDGEMENTS

The author would like to thank Mr. Takashi Matsumura, Manager of Building Engineering Department of Kansai Electric Power Company for his permission to present this paper; Mr. Takashi Kida, Manager of Architectural Department of NEWJEC for his assistance; and Mr. Takaaki Ikeda, Research Engineer and Mr. Baoqi Guan, former researcher of Technical Research Institute of Tobishima Corporation for their assistance in the analyses.

REFERENCES

Celebi, M., 1997. Response of Olive View Hospital to Northridge and Whittier Earthquakes, Journal of Structural Engineering, ASCE, Vol. 123, No. 4, pp. 389-396.

Kowada, A., Maeda, N., Mori, S., Ikeda, T. and Guan, B., 1998. Nonlinear behavior of a towering R/C smokestack on soft ground during the 1995 Hyogoken-Nanbu earthquake, Journal of Structural and Construction Engineering, Architectural Institute of Japan, No.512, pp.67-74. (in Japanese with English abstract)

Kida, T., Mori, S., Hara, E., Masubuchi, K., Mikuriya, K., and Yamakawa, M. 1992. Seismic design of 200 m high R/C smokestack constructed on soft ground and verification of used dynamic analysis model (Part 1) – (Part 6), Proceedings of the Annual Conference of Architectural Institute of Japan, Vol. Structure, pp. 493-504.

Kowada, A., Maeda, N., Mori, S., Ikeda, T., and Maekawa, Y. 1997. Verification of a dynamic design model of a high smokestack for the 1995 Great Hanshin earthquake motion records (Part 1) – (Part 3), Proceedings of the Annual Conference of Architectural Institute of Japan, Vol. Structure, pp. 351-356. (in Japanese)

Kowada, A., Maeda, N., Mori, S., Ikeda, T., and Guan, B. 1997. Behavior of a high smokestack under strong and weak ground motions analyses by earthquake observation records (Part 1) – (Part 3), Proceedings of the Annual Conference of Architectural Institute of Japan, Vol. Structure, pp. 357-362. (in Japanese)

Li, Y. and Mau, S. T., 1997. Learning from recorded earthquake motion of buildings, Journal of Structural Engineering, ASCE, Vol. 123, No. 1, pp. 62-69.

Luco, J. E., Trifunac, M. D. and Wong, H. L., 1987. On the apparent change in dynamic behavior of a nine-story reinforced concrete building, Bull, Seism. Soc. Am. , Vol. 77, No. 6, pp. 1961-1983.

Mori, S., Ikeda, T., Takaimoto, Y., Muto, M. and Tohaya, T. 1992. Influence of soil liquefaction on dynamic response of structure on pile foundation, Proceedings of the 10th World Conference of Earthquake Engineering, Madrid, Spain, Vol.3, pp.1777-1780.

Mori, S., 2000. Proposal of spring-mass model for pile-foundationed structure and its application to really damaged structures, Journal of Applied Mechanics, Japan Society of Civil Engineers, Vol.3, pp. 609-620. (in Japanese with English abstract)

Ohba, S. and Hamakawa, N., 1995. Change in predominant period of building due to damage to pile by the Hyogo-ken Nanbu earthquake, Journal of Architectural Institute of Japan, No.495, pp. 63-70. (in Japanese)

Penzien, J., Scheffey, C. F. and Parmelee, R. A. 1964. Seismic Analysis of Bridges on Long Piles, Proceedings of ASCE, Vol. 90, EM3, pp. 223-254.

Uchida, N., Ezaki, F., Matsunaga, K., Aoyagi, T, and Kawamura, M., 1980. Actual behavior of Sendai Building of Sumitomo Life Insurance under a strong motion – Part 1 Strong motion records during the Miyagi-ken Oki earthquake of February 20, 1978 and an elasto-plastic response analysis by using them, Journal of Architectural Institute of Japan, No. 290, 69-80. (in Japanese)

Uchida, N., Ezaki, F., Matsunaga, K., Aoyagi, T, and Kawamura, M., 1981. Actual behavior of Sendai Building of Sumitomo Life Insurance under a strong motion – Part 2 Strong motion records during the Miyagi-ken Oki earthquake of June 12, 1978 and an elasto-plastic response analysis by using them, Journal of Architectural Institute of Japan, No. 290, 69-80. (in Japanese)